High-performance materials for particles and supercritical CO_2 heat exchangers of next-generation concentrated solar power plant systems

Daniel Benitez,* Benedikt Kölsch, Tom Blackburn, Alexander Knowles, Kan Ma, Michael Kerbstadt, Emma White, Mathias Galetz, Tatu Pinomaa, Līva Freimane, Anssi Laukkanen, Marta Navas, and Rebeca Hernández

Received: 24 July 2025 / Revised: 5 December 2025 / Accepted: 9 December 2025

High-temperature heat exchangers for concentrated solar thermal systems operating at up to 750°C and 250 bar face challenges, including creep, oxidation, corrosion, thermal cycling, and particle-driven erosion. The COMPASsCO2 project explored Cr-based superalloys as cost-effective alternatives to conventional Ni-based alloys. Two novel material systems were developed: Cr-NiAl alloys with Fe additions that reached homogeneous microstructures and stable NiAl precipitates, enhancing high-temperature strength, and Cr-Si alloys showing exceptional hardness and erosion resistance. Although high ductile-to-brittle transition temperatures limited the use of Cr-Si as bulk materials, they proved effective as protective slurry coatings. A novel Cr-Si diffusion coating process was developed and validated through oxidation and erosion testing. Laboratory-scale testing under simulated conditions was supported by computational wear modeling, thermodynamic simulations, and machine-learning-based microstructural analysis. These findings highlight material solutions applicable to the particle/sCO_2 use case and relevant to other high-temperature, chemically aggressive industrial environments.

Impact statement

Decarbonizing high-temperature process heat and power demands materials that survive >750°C, high pressure, and particle flows. This study introduces new chromium-based alloys and protective coatings designed for the next generation of concentrated solar thermal power plants that use supercritical carbon dioxide and solid particles to convert heat into electricity more efficiently. The research combines advanced materials development with computer simulations and machine learning to predict how these materials perform over time. The newly developed chromium–nickel–aluminum and chromium–silicon materials show excellent resistance to heat, corrosion, and particle erosion at temperatures up to 900°C. A new, low-cost coating method provides durable surface protection and could extend the lifetime of heat exchanger components by a decade. Beyond solar energy, these findings are relevant for any high-temperature industry, such as gas turbines, hydrogen production, or chemical processing, where materials failure limits efficiency and sustainability. By improving durability and reducing maintenance costs, this work supports more affordable and reliable renewable energy systems and offers a pathway toward cleaner, longer-lasting technologies for high-temperature industrial applications.

Introduction

Concentrated solar thermal (CST) systems operating at temperatures above 750°C and pressures up to 250 bar pose severe material challenges, particularly for components such as heat exchangers that experience cyclic oxidation, corrosion, and erosion. Within the COMPASsCO2 project, one research focus was the development of high-performance materials capable of withstanding these extreme conditions. As CST technology advances, in this case with the integration of supercritical CO_2 (sCO_2) Brayton power cycle and solid particles serving as both heat transfer and thermal storage medium (schematic shown in **Figure** 1), the limitations of conventional heat exchanger materials have become increasingly evident. Nickel-based superalloys and austenitic steels, while offering good creep strength and oxidation resistance, exhibit performance

Daniel Benitez, German Aerospace Centre DLR, Institute of Solar Research, 04005 Almería, Spain; daniel.benitez@dlr.de
Benedikt Kölsch, German Aerospace Centre DLR, Institute of Solar Research, 51147 Cologne, Germany
Tom Blackburn, School of Metallurgy and Materials, University of Birmingham, Birmingham B15 2TT, UK
Alexander Knowles, School of Metallurgy and Materials, University of Birmingham, Birmingham B15 2TT, UK
Kan Ma, Department of Mechanical Engineering, City University of Hong Kong, Kowloon, Hong Kong, China
Michael Kerbstadt, Dechema-Forschungsinstitut, 60486 Frankfurt am Main, Germany
Emma White, Dechema-Forschungsinstitut, 60486 Frankfurt am Main, Germany
Mathias Galetz, Dechema-Forschungsinstitut, 60486 Frankfurt am Main, Germany
Tatu Pinomaa, VTT Technical Research Centre of Finland Ltd, 02044 Espoo, Finland
Līva Freimane, VTT Technical Research Centre of Finland Ltd, 02044 Espoo, Finland
Anssi Laukkanen, VTT Technical Research Centre of Finland Ltd, 02044 Espoo, Finland
Marta Navas, Materials of Energetic Interest Division, Technology Department, CIEMAT, Madrid, Spain
Rebeca Hernández, Materials of Energetic Interest Division, Technology Department, CIEMAT, Madrid, Spain
*Corresponding author
doi:10.1557/s43577-025-01049-9

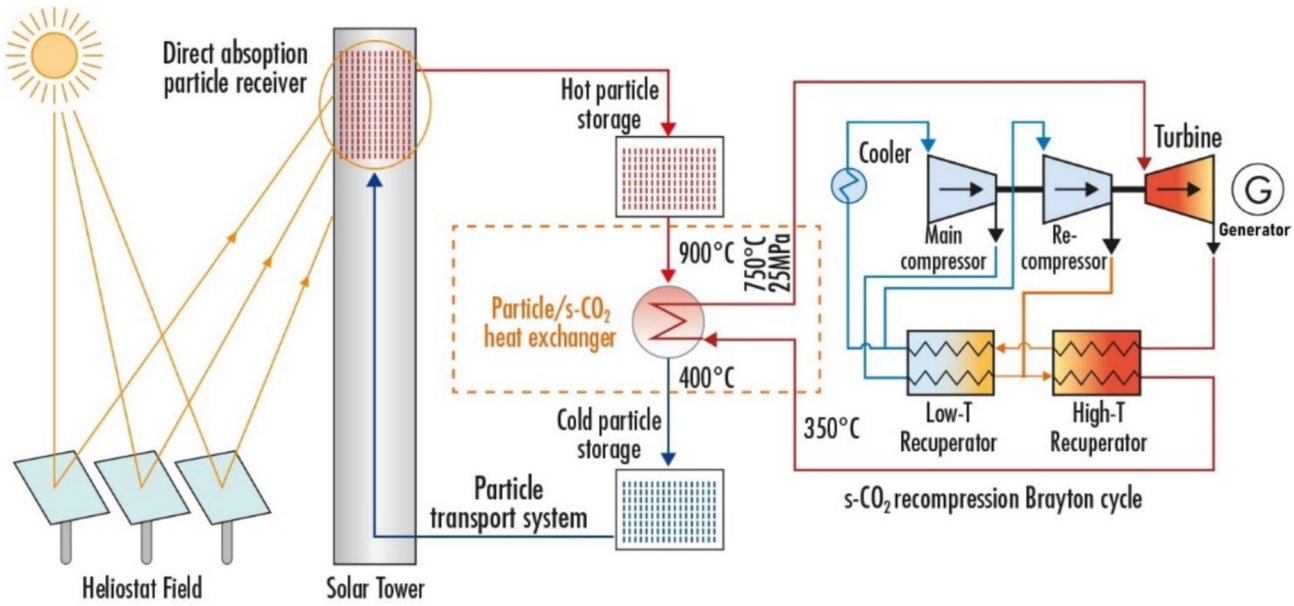

Figure 1. Schematic of a concentrated solar thermal plant with solid particles as heat transfer and storage medium, coupled with a supercritical CO_2 (sCO_2) Brayton power cycle and a particle/sCO_2 heat exchanger. Adapted with permission from Reference 1. © 2025 Wiley.

degradation above approximately 700°C. Consequently, there is growing interest in refractory-based alloys, which possess inherently high melting points exceeding <1900°C.

One promising approach explored in COMPASsCO2 involves the development of novel Cr-based alloys. Cr combines a high melting point (~1907°C) with excellent oxidation resistance and cost advantages compared to nickel or cobalt. However, its widespread use as a bulk material has been hindered by challenges such as nitridation-induced embrittlement as well as reduced oxidation resistance above 900°C.[2,3] Overcoming these challenges are key to enabling their use in next-generation CST heat exchangers. To this end, two alloy systems have been investigated:

1. Cr-based alloys strengthened by B2-NiAl precipitates, offering high-temperature strength and stability.
2. Cr strengthened by A15-Cr_3Si precipitates, enhancing oxidation and nitridation resistance.

In parallel, COMPASsCO2 has also developed advanced coatings designed to improve oxidation, corrosion, and erosion resistance of conventional heat exchanger tube materials.

Materials and methods

Benchmark materials

Following a detailed literature review conducted by Galetz et al.,[1] a representative set of state-of-the-art high-temperature materials was selected for benchmarking and assessment of their compatibility with next-generation CST plants using solid particles and sCO_2. These materials included nickel-based superalloys such as Inconel 617b (solid-solution strengthened), Inconel 740, and Haynes 282 (γ-γ′ based), along with the solid-solution nickel-based superalloy, the high-temperature austenitic steel Sanicro 25, and the ferritic steels P91 and 92. These alloys are commonly employed in thick-walled components of steam-cycle systems, including main steam pipework and superheater outlet headers, where they are subjected to creep, fatigue, and creep-fatigue loading.[4] The compatibility of Sanicro 25, Inconel 625, Inconel 740, and Haynes 282 in sCO_2 environments and their oxidation test results at different temperatures and exposure times are reported in References 5 and 6.

Initial microstructural characterization of the commercial alloys was conducted using optical and scanning electron microscopy (SEM), complemented by hardness measurements. Tensile testing was conducted across a temperature range from room temperature (RT) to 900°C to evaluate the mechanical performance of the reference alloys. These results established a reference for comparison with newly developed materials and guided subsequent alloy design and selection.

Development of novel Cr-based alloys

Novel Cr-based body-centered-cubic (bcc) superalloys based on the Cr-NiAl system represent an innovative alternative to high-temperature materials.[7,8] Bcc superalloys are a new class of high-temperature materials comprising a disordered-bcc matrix (β) and ordered-bcc precipitates (β′).[9] Their β-β′ microstructure design mirrors the γ-γ′ microstructure of nickel superalloys. They offer exceptional strength retention at temperatures exceeding 1200°C, surpassing conventional

Table I. Material properties used in the particle/s-CO_2 heat exchanger tube bundle wear simulations.

	Density (kg/m^3)	Young's Modulus (GPa)	Poisson's Ratio	Yield Strength (MPa)
Particles	3500	319	0.20	–
Heat exchanger tube	7800	200	0.29	450

nickel-based superalloys. Their bcc crystal structure provides inherent high-temperature strength and creep resistance, making them promising candidates for next-generation turbine engines and power generation systems.[10,11] However, these alloys face significant challenges including poor oxidation resistance at elevated temperatures and brittleness at room temperature.[12] Samples of different alloys were produced by melting high-purity Cr, Ni, Al, and Fe in an arc-melter under Argon in order to leverage a dual-phase microstructure consisting of a ductile bcc-Cr matrix (β-phase) reinforced by nanoscale, ordered bcc-B2 NiAl precipitates (β′-phase).

Prior studies have shown that silicon additions play a crucial role in enhancing the oxidation and nitridation resistance of chromium-based alloys. Experiments conducted in synthetic air at 1200°C for 1000 h demonstrated that even small additions of Si (3 at.%) significantly reduce Cr_2O_3 volatility and suppress internal nitridation through stabilization of Cr_3Si, which effectively resists nitrogen penetration. At higher Si contents (≥8 at.%), the formation of protective SiO_2-Cr_2O_3 scales further improves environmental resistance.[13] Additional alloying with elements such as Ge, Pt, and Mo was found to further improve the oxidation and nitridation resistance.[9,10] In order to study its mechanical properties, Cr-Si alloys were synthesized, combining a Cr solid solution (Cr_{ss}) matrix containing A15-structured Cr_3Si silicide precipitates. Silicon additions were selected for their ability to promote the formation of stable oxides and nitrides, improving oxidation and nitration resistance. The Cr_3Si phase contributes to increased strength and hardness, further enhancing high-temperature performance.

Development of Cr-Si diffusion coatings

A novel Cr-Si diffusion coating process was developed and patented using a novel slurry coating technique, applicable to both steels and nickel-based superalloys.[14–16] Compared with the state-of-the-art pack cementation process, this innovative slurry process offers notable economic and practical advantages, particularly for large-scale components such as intended heat exchanger tubes. This method involves air-brushing Cr-Si-rich slurries onto metal substrates, followed by thermal diffusion treatments in a controlled atmosphere. This process generates a Cr- and Si-enriched outer diffusion layer capable of forming a protective and long-lasting Cr_2O_3 scale during high-temperature exposure. Additionally, the incorporation of Si promotes the precipitation of intermetallic silicide within the diffusion layer, thereby enhancing surface hardness and improving the coating erosion resistance. The hardnesses of the coatings were determined by microhardness measurements using the Vickers method with a LEICA VMHT MOT hardness tester. Erosion testing of coated Sanicro 25 was performed for 250 h at 900°C using a rotating holder operating at 5 $mm.s^{-1}$ in a particle bed. Cross-sectional SEM analysis was performed to determine possible wear of the coating layer.

Wear simulation of particle–tube interactions

Long-term material degradation can be determined using computational wear simulations based on the discrete element method (DEM),[17] and is implemented via the open-source software LIGGGHTS.[18] The model was adapted to simulate a particle–tube interaction environment within a representative heat exchanger geometry consisting of five staggered tube rows. Boundary conditions were applied such that particle inflow and outflow occurred in the vertical direction by gravity, while periodic boundary conditions were imposed

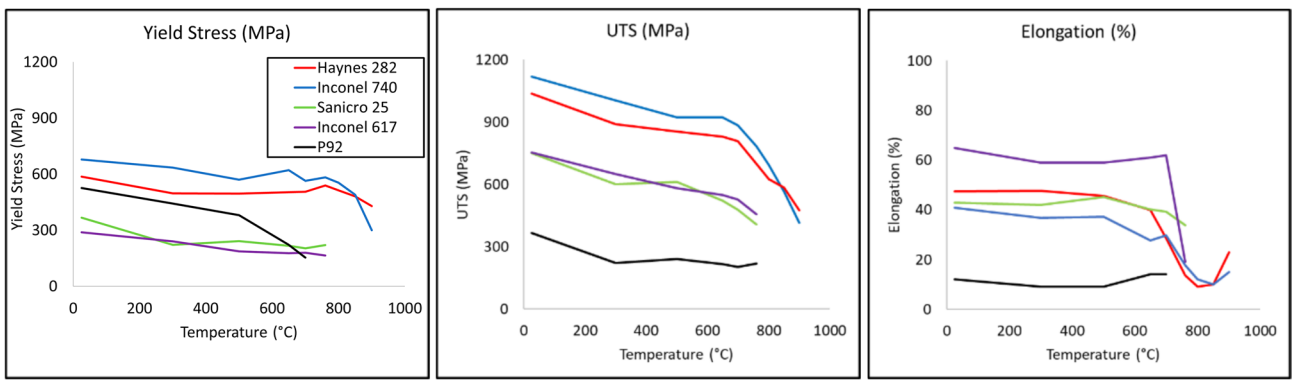

Figure 2. Tensile parameters (yield stress [MPa], ultimate tensile strength [UTS, MPa] and elongation [%]) obtained between room temperature and 760°C/900°C on state-of-the-art materials.

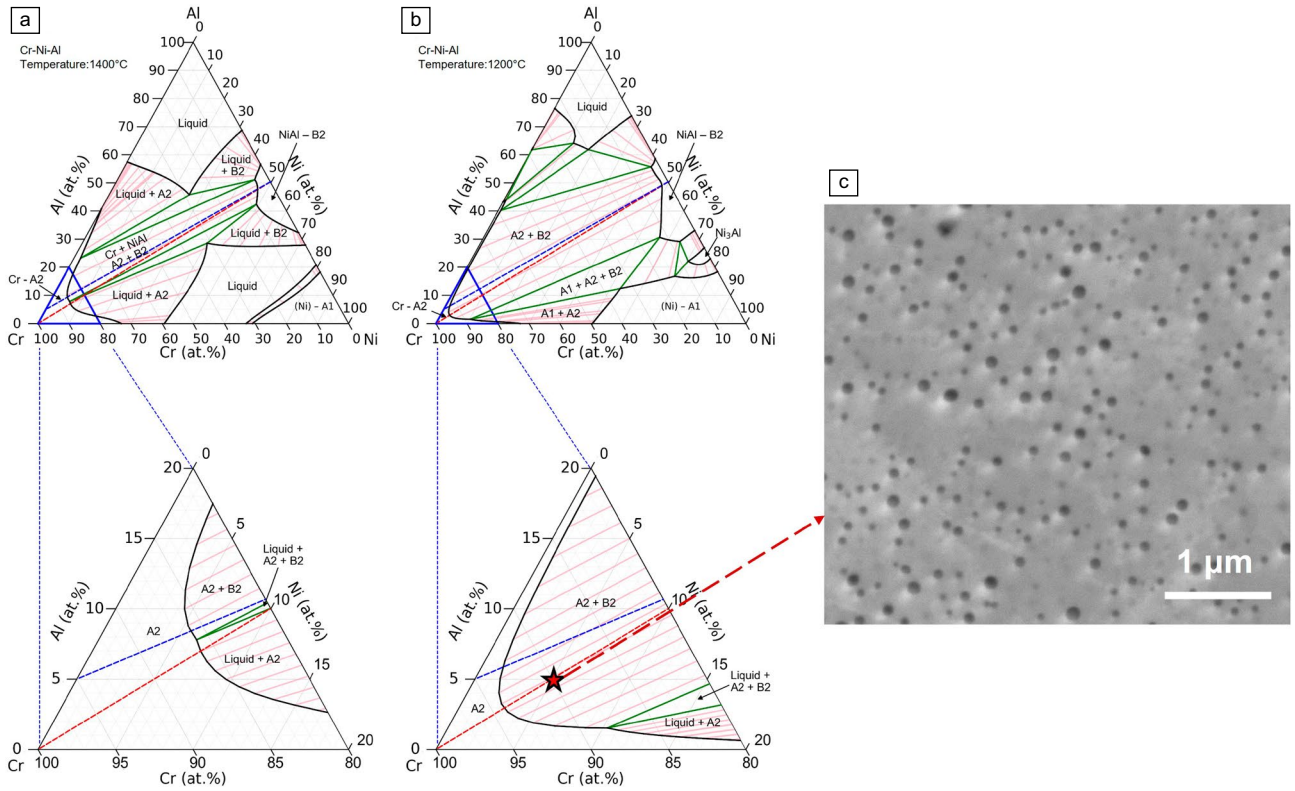

Figure 3. Cr-Ni–Al ternary phase diagram displayed at (a) 1400 and (b) 1200°C with higher magnification insets of the chromium-rich corner highlighting the narrow single-phase region that shrinks significantly with reducing temperature. Calculated using the TCHEA-8 database in Thermocalc. (c) Scanning electron microscopy micrograph showing the microstructure of the Cr-5Ni-5Al (atomic percent) alloy after homogenization at 1400°C for 20 h and aging at 1200°C for 4 h, creating a β-β′ microstructure.

on the remaining axes. Particle trajectories were tracked using Lagrangian mechanics, and the Finnie wear model was employed to estimate material removal. The number of particles entering the system was scaled to a representative particle mass flow rate per inlet area, assuming a particle diameter of 1 mm. Material properties of the particles and heat exchanger tube structural materials used in the simulation are listed in **Table** I.

Results

Characterization and mechanical testing of state-of-the-art materials

Tensile tests from room temperature (RT) to 900°C revealed distinct trends among the investigated materials (**Figure** 2). Up to 760°C Inconel 740 (IN740) exhibited the highest yield stress across the entire temperature range, while Haynes 282 and Inconel 617 (IN617) demonstrated superior ductility, as indicated by their greater elongation to failure. Below 600°C, the ferric steel P92 provided the best balance of strength and ductility, reflected in its balanced tensile stress-to-elongation ratio. The results are consistent with the mechanical stability expected for these materials at high temperatures.

At ultrahigh temperature (≥800°C), IN740 maintained a high yield stress and ductility compared to Haynes 282. Nonetheless, both alloys exhibit notable strength degradation above 850°C. At 900°C, Haynes 282 marginally outperformed IN740 in terms of tensile stress. This temperature-depending decline underscores the operational temperature limits of nickel-based superalloys in extreme CST environments. Overall, these results indicate that Haynes 282 is more suitable for applications approaching 900°C, whereas IN740 offers robust performance at intermediate temperatures.

Cr-NiAl bcc superalloys: Developments and challenges

A fundamental study on the Cr-Ni–Al ternary system was conducted, focusing on the solubility behavior of the B2 phase (NiAl) within the A2-Cr. **Figure** 3a–b shows the ternary phase diagrams at 1400 and 1200°C. They demonstrated that Cr-Ni–Al systems at the chromium-rich corner can be solution heat-treated at a high temperature (such as 1400°C) and aged heat-treated at lower temperatures. Figure 3c presents a typical Cr-NiAl superalloy microstructure achieved after homogenization and aged at 1200°C for 4 h. The spherical precipitates are B2-NiAl embedded in a Cr matrix with trace Ni and Al. It results in a high microhardness of ~570 $HV_{0.5}$, significantly improved compared to the pure Cr of ~180 $HV_{0.5}$.

In this work, a key issue of the Cr-NiAl bcc-superalloy is identified: the limited solubility of NiAl within Cr. As

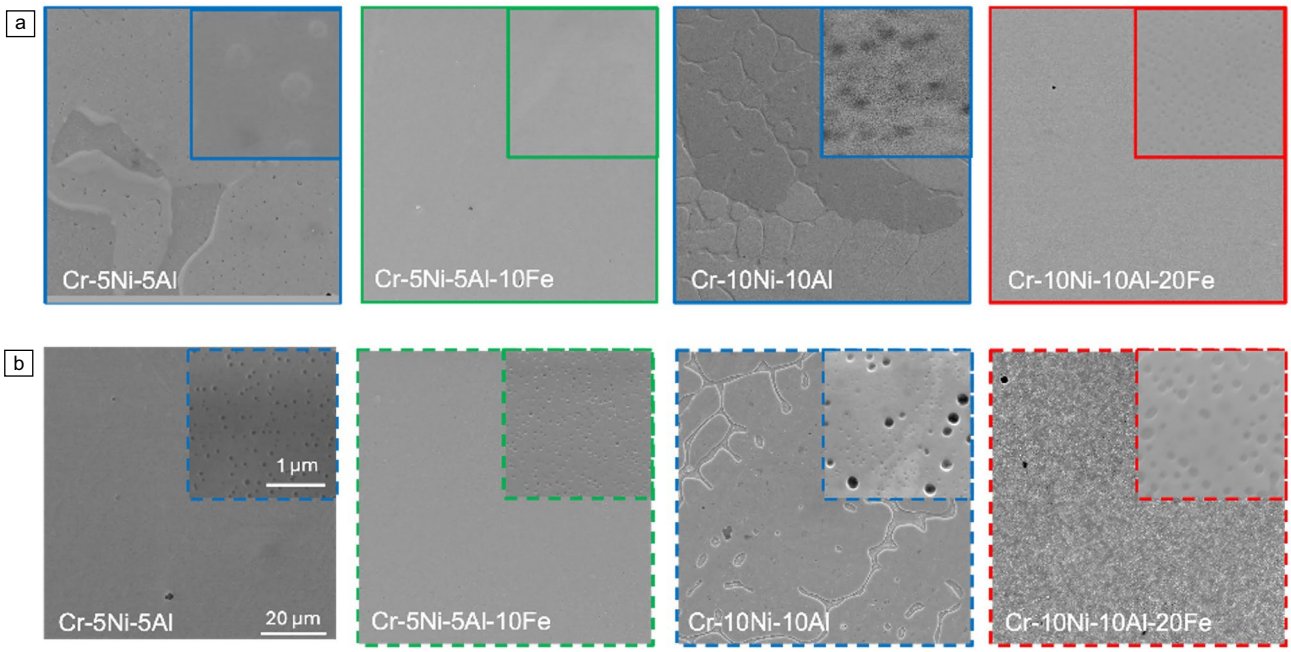

Figure 4. Scanning electron microscopy micrograph showing the microstructure of Fe-free and Fe-contained Cr-NiAl body-centered-cubic superalloys (a) after homogenization at 1400°C for 20 h and (b) aging at 1000°C for 20 h. Inset figures showing magnified microstructure.

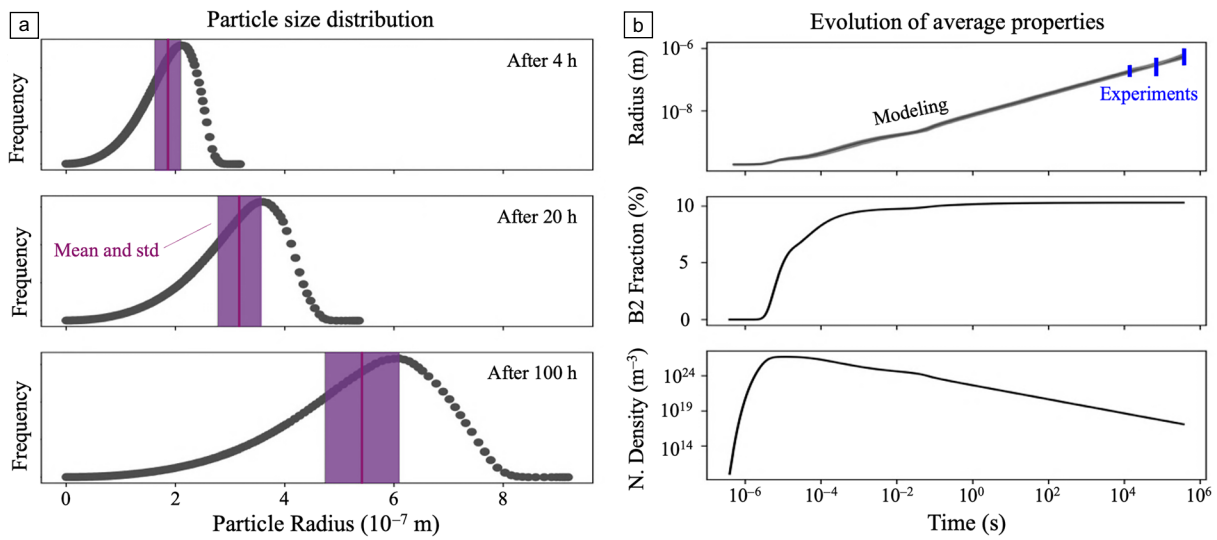

Figure 5. Precipitation simulations for Cr-based body-centered-cubic superalloy (Cr-5Ni-5Al-20Fe), showing (a) the precipitate particle size distribution after 4, 20, and 100 h. The average particle size was fitted to experimentally acquired average particle size, and (b) evolution of average properties during precipitate coarsening. Adapted with permission from Reference 21. © 2023.

shown in **Figure** 4, the alloy with an addition of 5Ni and 5Al (atomic percent) could not be homogenized at 1400°C. However, alloying with Fe was found to increase solubility. This was epitomized by the fact that compared to the ternary systems (Cr-5Ni-5Al and Cr-10Ni-10Al) that produced dendritic NiAl upon heat treatment at 1400°C for 20 h, additions of 10 and 20 at.% Fe respectively alleviated the dendritic NiAl at 1400°C allowing a fully homogeneous microstructure to be achieved. This is seen as a crucial requirement for the design of bcc-superalloys to allow controlled and uniform precipitate growth. Cr-based alloys exhibit an ultralow matrix-precipitate lattice misfit (~0.1%), leading to a coherent matrix–precipitate interface and explaining the spherical morphology of precipitates.[19] The coarsening of these precipitates was studied using a new machine learning (ML)-based image analysis method to accelerate microstructure investigation, namely precipitate

size measurements,[20] and showed coarsening rates as low as ~10^2 nm^3/h at 1000°C—orders of magnitude below conventional superalloys.

To complement the experimental findings, a precipitation-kinetics model was developed and applied to the Cr-5Ni-5Al-20Fe alloy using Thermo-Calc's Precipitation Module, shown in **Figure** 5. The model was calibrated against experimental coarsening data[19] to determine the matrix–precipitate interface energy. A low interfacial energy of 0.02 $J.m^{-2}$ at 1200°C was obtained for bcc A2-B2 phases, indicating a relatively low coarsening rate and thus microstructural stability of the alloy at elevated temperatures. The simulations predict the time-dependent evolution of precipitate size, volume fraction, and composition, offering a valuable tool for guiding alloy design and heat treatment strategies.

Cr-Si-(Fe/Ni) alloys: Advantages and challenges

The effect of Ni and Fe additions on the microstructure and mechanical properties of Cr-Si alloys was systematically investigated. These alloys inherently combine exceptional high-temperature strength, erosion resistance, and phase stability, making them promising candidates for harsh thermal environments. The addition of Fe (≤16 at.%) was found to enhance solid-solution hardening, resulting in an approximate 35% increase in microhardness. Ni additions (≤32 at.%) led to the formation of the σ-phase ($Cr_{13}N_{15}S_{12}$), achieving a peak hardness of 1080 $HV_{0.3}$.

However, brittleness remains a critical limitation of these alloys despite maintaining sufficient Si content to stabilize protective barriers. Fe-modified alloys show ductile-to-brittle transition temperatures (DBTTs) in the range of 600–700°C, while Ni-containing variants show even higher DBTTs, exceeding 700°C. The embrittlement in Ni-containing alloys is primarily attributed to the formation of the σ-phase. Additionally, excessive Ni contents promote the formation of soft, face-centered- cubic Ni-rich precipitates, reducing the overall hardness.

Achieving an optimal balance between silicide volume fraction and matrix ductility is therefore a key objective for future alloy design. While the high DBTTs restrict the use of Cr-Si-Fe/Ni alloys as bulk materials, their hardness and environmental durability make them highly promising as erosion-resistant coatings for conventional Fe/Ni substrates.

Novel Cr-Si slurry coatings for aggressive environments

The innovative slurry coating technique that produces a 50–150-µm-thick diffusion layer enriched with Cr and Si was successfully applied to Fe-based and Ni-based alloys. Long duration (quasi-)isothermal oxidation exposures at 900°C for 1000 h in laboratory air, particularly relevant to the outer surface of the heat exchanger tubes, showed a superior oxidation resistance for Cr-Si slurry-coated nickel-based superalloys compared to their uncoated counterparts as published and analyzed in detail in Reference 15. In particular, Inconel 740H and Rene 80 exhibited increasing detrimental internal oxidation of Al beneath an external Cr_2O_3 scale over time, the coated specimens formed an additional Si-rich subscale due to the incorporation of Si into the diffusion layer. This Si-enriched subscale acts as an effective diffusion barrier and prevents internal corrosion products from occurring and lowers the mass gain compared to the uncoated alloy.[15]

Table II. Comparison of hardness values for Cr-Si slurry coatings and base alloys: Sanicro 25, Inconel 617b, and P92 (all values in HV 25 and measured after the individual coating heat treatment process).

	Sanicro 25	Inconel 617b	P92
Base alloy (HV 25)	179 ± 53	404 ± 26	370 ± 13
Cr-Si slurry coated (HV 25)	884 ± 63	1149 ± 112	552 ± 39

In the present work, the erosion resistance of the Cr/Si slurry coatings is presented. Here, the influence of flowing heat carrier particles on the coating performance is investigated, complementing the previously reported oxidation-focused studies. Microhardness (HV 25) measurement results are presented in **Table** II. Due to the incorporation of Si and the precipitation of Si-rich intermetallics (e.g., $Cr_{13}Ni_5Si_3$ in Inconel 740H)[15] the Cr-Si slurry coatings exhibited hardness increases of approximately 50% for P92, more than 150% for Inconel 617b, and almost 400% for Sanicro 25, all measured after the respective heat treatment process of the coating. The pronounced increase in hardness is expected to contribute beneficially to the erosion resistance required in the targeted heat exchanger environment.

Erosion testing of Cr-Si coated Sanicro 25 for 250 h at 900°C in a sample holder rotating in a particle bed at 5 mm. s^{-1} showed excellent erosion resistance of the Cr-Si diffusion coating (**Figure** 6). After exposure, the formed Cr_2O_3 scale remained intact and was not eroded by the flowing particles, exhibiting only a few minor surface cracks (Figure 6b). Instead, particle wear product was observed to deposit on the oxide scale, as evidenced by aluminum and oxygen elemental maps (Figure 6c). This deposition indicated the high adherence of the chromia scale to the substrate and the high hardness of the interdiffusion zone. The combination of oxidation stability, mechanical robustness, and scalability,makes this Cr-Si slurry coating process a promising and sustainable surface protection strategy for extend component lifespans in extreme environments, especially those located on the exterior surfaces of a particle/s-CO_2 heat exchanger for next-generation CST systems.

Cylindrical specimens of Haynes 282 and P92, both coated and uncoated, were tested in a rotating multisampling holder at 700°C surrounded by "FerOx" particles, developed in the project COMPASsCO2, as the erosive medium. Two rotation velocities were applied (5 and 20 mm/s), and the samples were mounted in a tubular geometry allowing exposure of four circumferential positions: front (direct particle impact), backside,

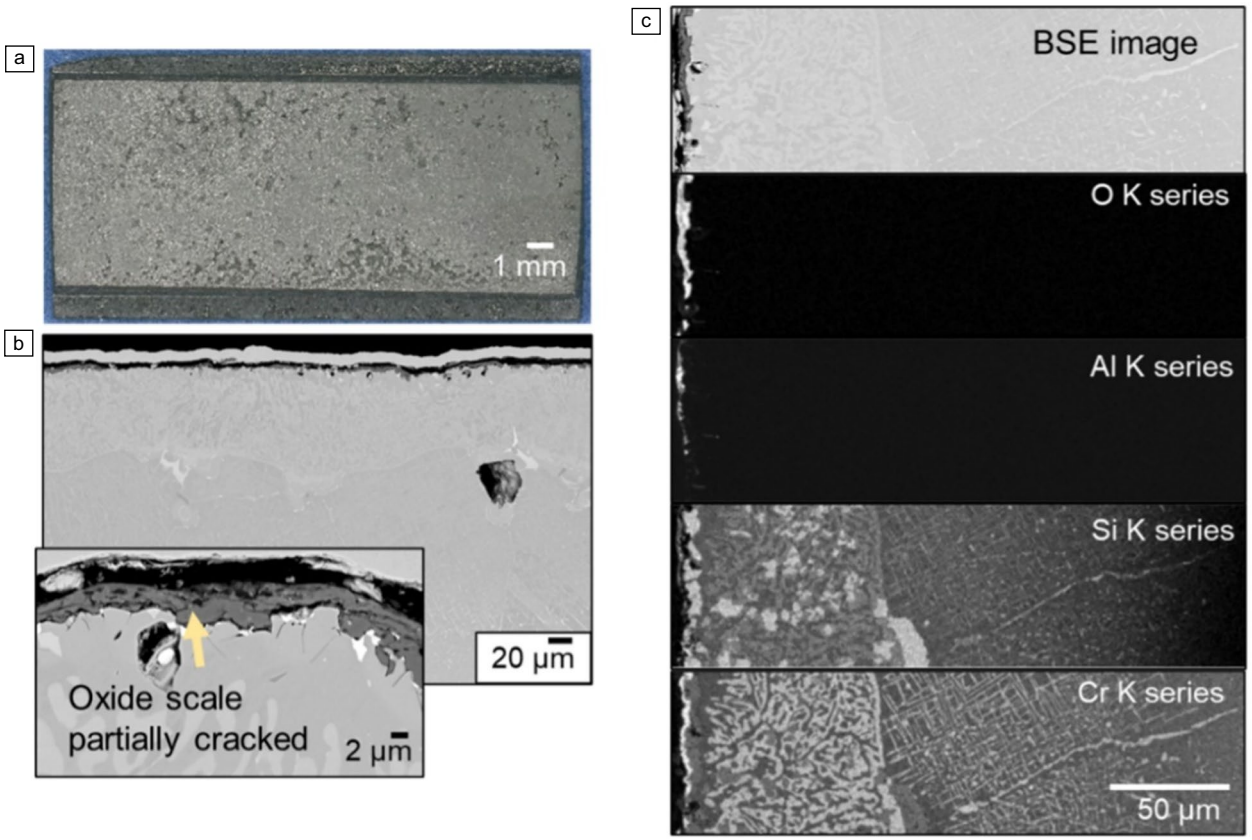

Figure 6. (a) Optical image of Cr-Si-coated Sanicro 25 after erosion testing for 250 h in laboratory air at 900°C using FerOx 16/30 granulate and rotation at 5 $mm.s^{-1}$. (b) Scanning electron microscopy (SEM) imaging of the cross section. (c) SEM/EDS elemental maps of the cross section. BSE, backscattered electron; EDS, energy-dispersive x-ray spectroscopy.

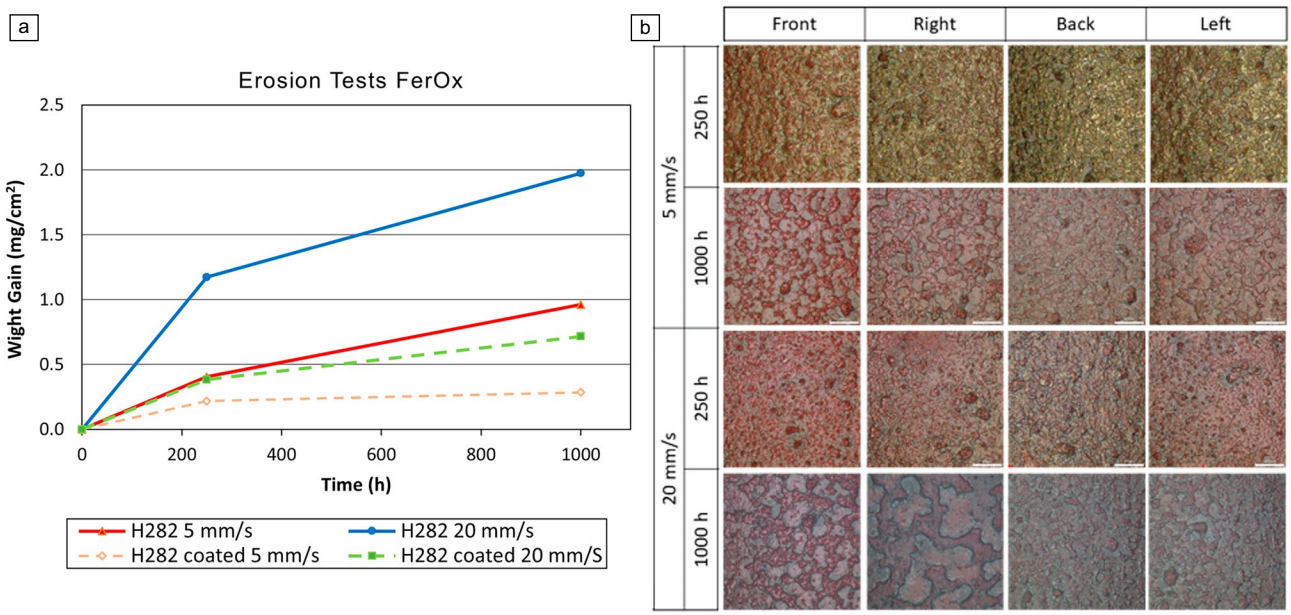

Figure 7. Effect of particle velocity on the erosion tests of Haynes 282 at 700°C. (a) Weight gain measurements of uncoated and coated samples. (b) Optical microscope images of the surface appearance at different times of the coated Haynes 282.

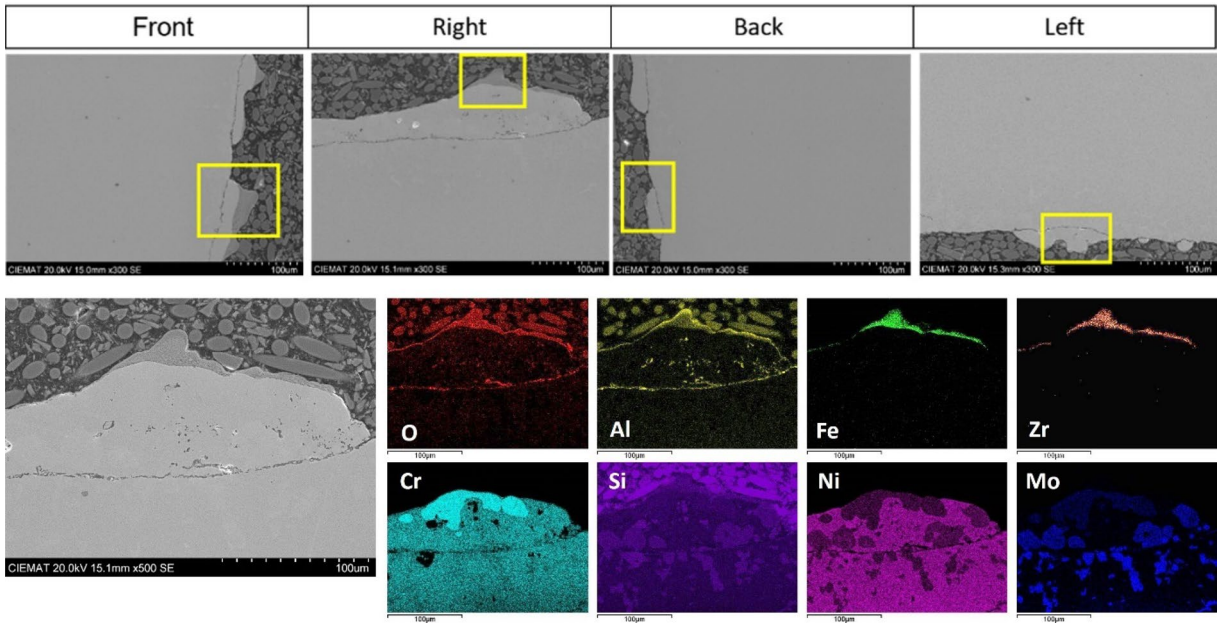

Figure 8. Scanning electron microscopy/EDX cross section of coated Haynes 282 specimen tested at 20 mm/s during 1000 h (top) at the different sides of the tubular specimen and (bottom) EDX analyses of the deposit, coating and base material in the lateral right side of the specimen.

and two lateral sides. This configuration enabled systematic study of particle impact angle and erosion morphology. Coated Haynes 282 demonstrated a good erosion resistance, maintaining coating integrity throughout testing (**Figure** 7). While particles deposition occurred on both coated and uncoated surfaces, the extent of deposition was influenced by the particle velocity and exposure time.

Cross-sectional SEM examinations indicate that the coating layers remain intact after testing, showing no signs of erosion degradation (**Figure** 8). Instead, particle deposits accumulated preferentially on the external lateral sides, where impact frequency and kinetic energy were highest. The outer deposits consisted primarily of Fe, O, Al, Si, and Zr. The shape of the deposits on the most exposed sides demonstrated that the impact of particles produced a characteristic wave-like morphology, indicative of wear/erosion degradation. This morphology has not been observed on the backside, where direct impact was minimal. Importantly, no delamination or cracking of the coating was observed beneath the deposits, confirming its excellent adhesion and erosion resistance. Si and Cr diffusion is also determined in the Haynes 282 base metal. Therefore, the beneficial effect of the coating on Haynes 282 was demonstrated by the lowest weight gain, which is consistent with the lower particle deposition and no oxide growth.

Experimentally calibrated computational wear prediction framework

A computational wear-prediction framework was developed, illustrated in **Figure** 9, to simulate particles-induced erosion within a representative CST heat exchanger geometry and to extrapolate wear behavior over extended operational times. The DEM model tracked particle flow and collision dynamics over a total physical time of 13.5 s. Following key measures, such as velocity distributions and local wear rate, the simulation reached a representative "steady-state" flow condition after approximately 10 s in the simulated heat exchanger. Beyond this point, both the wear volume and particle velocity distributions increased linearly with time, while fluctuations are visible due to stochastic particle impacts. The wear tends to accumulate to the upper diagonal regions of each tube rather than at the tube top center (zenith) position, as seen in Figure 9a. The average wear rate of each tube, shown in Figure 9b, exhibits nearly identical temporal behavior across the tube rows. The observed vertical offsets in the curves correspond to the delayed arrival of particles at lower tubes. The linearized average wear rate (Figure 9c) was estimated to be approximately 0.520 $g.m^{-2}$ per year, which is used to calibrate the wear fit, shown in Figure 9d. Finally, the wear depth is predicted up to 10 years (Figure 9e).

Discussion

The development of Cr-based bcc superalloys strengthened by NiAl intermetallic precipitates represents a promising route toward next-generation high-temperature materials for CST applications. Within the COMPASsCO2 project, the addition of Fe into Cr-NiAl alloys has been identified as a solution to increase the solubility of NiAl in the Cr matrix. This can improve the volume fraction of the precipitates, leading to potential benefits of high-temperature

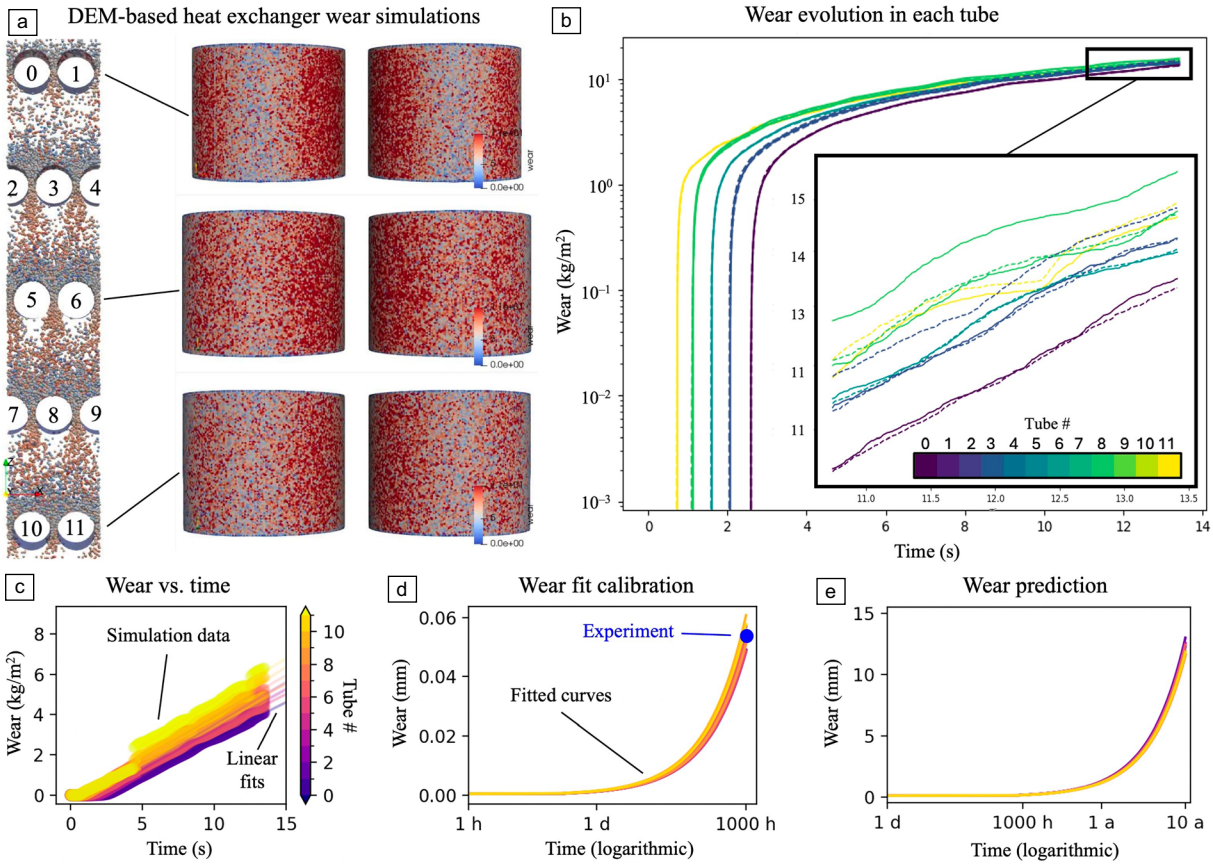

Figure 9. Overview of the computational concentrated solar thermal (CST) heat exchanger wear simulation framework, consisting of (a) discrete element method (DEM-based particle/tube bundle simulations, (b) average wear volume for each tube row, (c) wear over time with linear extrapolation, (d) calibration to 1000 h wear test, and (e) prediction of wear into the future.

strength and creep resistance. The Cr(Fe)-NiAl system demonstrated a stable microstructure at high temperatures, similarly as in other bcc superalloys.[22] These features mark a significant advancement beyond conventional Ni-based alloys. Moreover, the ultralow matrix-precipitate lattice misfit (~0.1%) promotes coherent precipitation of nanoscale NiAl, which contributes to the observed mechanical stability. However, the ductility issue of these alloys should be addressed.

However, several challenges remain that currently preclude direct industrial application. Notably, the brittleness of these alloys below 450°C limits their thermal cycling resilience, which is critical for realistic CST operation. In addition, the long-term oxidation and corrosion behavior in both air and supercritical CO_2 environments is not yet fully characterized. Previous studies (e.g., by Locq et al.[8]) revealed internal oxidation under cyclic conditions in high NiAl volume fraction systems. In contrast, the present system features a lower volume fraction of NiAl and the addition of Fe, which could mitigate such effects. These alloys are expected to show improved oxidation resistance over pure Cr. However, it remains under investigation if these modifications enable the formation of protective alumina or chromia scales under CST-relevant conditions.

Ongoing work is underway to assess the performance of this novel material class under high-temperature exposure in both synthetic air and CO_2 environments. Current work aims to establish this understanding and provide a platform for future development of Cr-based bcc superalloys. In terms of CO_2 exposure, to the authors knowledge, no investigations have focused on the exposure on Cr strengthened by NiAl precipitates. Collaborative work initiated in the COMPASsCO2 framework will seek to investigate and provide better understanding of the performance of Cr-based alloys under CO_2 and other environments.

Beyond their application as protective coatings for CST, Cr-based coatings are particularly advantageous in high-temperature corrosion environments, such as those found in gas turbines. Therefore, the resistance of a novel Cr-Si slurry coating applied to Rene 80 against sodium sulphate (Na_2SO_4)-induced corrosion at 900°C was investigated.[16] Compared to the uncoated base alloy and a Cr coating applied via the pack cementation process, the Cr-Si slurry coating demonstrated significantly superior hot corrosion resistance. These results highlight its

broad applicability in harsh environments and its high technical relevance.

The wear simulation framework developed in the project adds an important predictive capability for lifetime estimations of heat exchanger components under realistic particle flow conditions. By calibrating the model to experimental erosion data, it enables extrapolation of material wear over service lifetimes of up to 10 years.

Conclusions

This work presents the development, characterization, and evaluation of novel Cr-NiAl and Cr-Si-based superalloys, as well as Cr-Cr_3Si slurry coatings, developed within the framework of the H2020 project COMPASsCO2.

The Cr-NiAl systems were found to exhibit a low solubility of NiAl within the Cr matrix. However, the addition of 10 and 20 at.% Fe enabled the formation of fully homogeneous microstructures. These uniform structures allow for the controlled precipitation of coherent nanoscale NiAl particles with spherical morphology, facilitated by the ultralow matrix-precipitate lattice misfit. To support alloy development, a new ML-based image analysis method was developed, significantly accelerating precipitate size measurements and enabling faster alloy optimization.

For Cr-Si alloys, the effect of Ni and Fe additions on microstructure and mechanical properties was systematically investigated. These alloys exhibit exceptional high-temperature strength, erosion resistance, and phase stability. However, their application as bulk structural materials remains limited by high ductile-to-brittle transition temperatures. As a solution, Cr-Si-Fe/Ni alloys were successfully applied as erosion-resistant coatings on conventional Fe/Ni substrates. A novel slurry-based Cr-Si diffusion coating process was developed, resulting in higher durability with enhanced resistance to oxidation and erosion at higher temperatures.

In order to estimate the long-term material performance, a wear simulation model based on the DEM was developed and experimentally calibrated using erosion-test data. This model was used to predict the wear behavior of heat-exchanger materials under particle-laden flow conditions, predicting operational lifetimes of up to 10 years (e.g., for IN740).

The results demonstrate that the novel material systems, including advanced Cr-based superalloys and coatings, can effectively withstand the harsh thermal, mechanical, and chemical environments present in particle/sCO_2 heat exchangers. These findings support the feasibility of deploying such materials in next-generation CST plants with sCO_2 Brayton cycles, contributing to more durable and efficient solar thermal systems.

Follow-up projects will focus on scaling up production, validating cost-effective production of these new materials, and investigating broader applications in other high-temperature, corrosive, and erosive industrial environments.

Author contributions

Study conception and design were done by D.B., B.K., A.K., K.M., T.B., and T.P. Material preparation, data collection, and analysis were performed by D.B., T.B., A.K., K.M., M.K., E.W., T.P., L.F., A.L., M.N., and R.H. The first draft of the manuscript was written by D.B. and all authors commented on previous versions of the manuscript. All authors read and approved the final manuscript.

Funding

Open Access funding enabled and organized by Projekt DEAL. This work is based on the results of the project COMPASsCO2 that received funding from the European Union's Horizon 2020 Research and Innovation Programme under Grant Agreement No. 958418 (https://www.compassco2.eu).

Data availability

Data sets generated during the current study are available from the corresponding author on reasonable request.

Competing interests

The authors have no competing interests to declare that are relevant to the content of this article.

References

1. M.C. Galetz, E.M.H. White, M. Kerbstadt, C. Schlereth, X. Montero, D. Benitez, *Adv. Eng. Mater.* **27**(10), 2402060 (2025). https://doi.org/10.1002/adem.202402060
2. W.D. Klopp, J.R. Stephens, *Ductility Mechanisms and Superplasticity in Chromium Alloys* (NASA Technical Note No. NASA-TN-D-4346z, NASA, Washington, DC, 1968)
3. M.P. Brady, J.H. Zhu, C.T. Liu, P.F. Tortorelli, L.R. Walker, *Intermetallics* **8**(9), 1111 (2000)
4. A. Di Gianfrancesco, R. Blum, "A-USC Programs in the European Union," in *Materials for Ultra-Supercritical and Advanced Ultra-Supercritical Power Plants,* ed. by A. Di Gianfrancesco (Elsevier, Amsterdam, 2017), chap. 24, pp. 773–846. https://doi.org/10.1016/B978-0-08-100552-1.00024-5
5. B.A. Pint, *Electrochem. Soc. Interface* **30**, 67 (2021). https://doi.org/10.1149/2.F07212IF
6. B.A. Pint, K.A. Unocic, R.G. Brese, J.R. Keiser, *Mater. High Temp.* **35**, 39 (2018). https://doi.org/10.1080/09603409.2017.1389371
7. Ö. Doğan, X. Song, D. Palacio, M. Gao, *J. Mater. Sci.* **49**, 805 (2014). https://doi.org/10.1007/s10853-013-7763-1
8. D. Locq, P. Caron, C. Ramusat, R. Mévrel, *Mater. Sci. Eng. A* **647**, 322 (2015). https://doi.org/10.1016/j.msea.2015.09.033

9. A.J. Knowles, C.H. Zenk, *Scr. Mater.* **267**, 116761 (2025). https://doi.org/10.1016/j.scriptamat.2025.116761
10. Q. Wang, Z. Wang, R. Wang, A.J. Knowles, C.H. Zenk, G. Song, C. Lee, P.K. Liaw, T. Wang, *Scr. Mater.* **267**, 116748 (2025). https://doi.org/10.1016/j.scriptamat.2025.116748
11. K. Ma, S. Cheng, X. Ma, T. Blackburn, A.J. Knowles, K. An, J. Santisteban, F. Sun, C.H. Zenk, P.A. Ferreirós, *Scr. Mater.* **267**, 116802 (2025). https://doi.org/10.1016/j.scriptamat.2025.116802
12. A. Kauffmann, B. Gorr, M. Heilmaier, *Scr. Mater.* **267**, 116784 (2025). https://doi.org/10.1016/j.scriptamat.2025.116784
13. A. Soleimani Dorcheh, M. Galetz, *Oxid. Met.* **88**, 549 (2017). https://doi.org/10.1007/s11085-016-9685-1
14. M. Kerbstadt, M. Galetz, *German Patent Application* **10**, 112 (2022)
15. M. Kerbstadt, E.M.H. White, M.C. Galetz, *Materials* (Basel) **16**, 7480 (2023). https://doi.org/10.3390/ma16237480
16. M. Kerbstadt, K. Ma, E.M.H. White, A.J. Knowles, M.C. Galetz, *High Temp. Corros. Mater.* **101**, 1077 (2024). https://doi.org/10.1007/s11085-024-10257-8
17. K. Kant, R. Pitchumani, *Solar Energy Mater. Sol. Cells.* **266**, 112629 (2024)
18. C. Kloss, C. Goniva, A. Hager, S. Amberger, *Prog. Comput. Fluid Dyn.* **12**(2/3), 140 (2012)
19. K. Ma, T. Blackburn, J.P. Magnussen, M. Kerbstadt, P.A. Ferreirós, T. Pinomaa, C. Hofer, D.G. Hopkinson, S.J. Day, P.A. Bagot, M. Moody, M.C. Galetz, A.J. Knowles, *Acta Mater.* **257**, 119183 (2023). https://doi.org/10.1016/j.actamat.2023.119183
20. Z. Xia, K. Ma, S. Cheng, T. Blackburn, Z. Peng, K. Zhu, W. Zhang, D. Xiao, A.J. Knowles, R. Arcucci, *Phys. Chem. Chem. Phys.* **25**, 15970 (2023). https://doi.org/10.1039/D3CP00402C
21. T. Pinomaa, L. Linnala, M. Tahkola, A. Laukkanen, M. Kerbstadt, C. Oskay, E. White, M. Galetz, K. Ma, T. Blackburn, S. Knowles, Correlated Modelling-Microstructure-Mechanical Property Understanding of the New Materials (Version 1), *Zenodo* (2023). https://doi.org/10.5281/zenodo.10174317
22. R.J. Vikram, S. Sen, L. Yang, M.K. Eusterholz, A. Radi, D. Schliephake, J. Couzinié, A. Kauffmann, M. Heilmaier, *Scr. Mater.* **271**, 117026 (2026). https://doi.org/10.1016/j.scriptamat.2025.117026